Marine Biotechnology (2023) 25:1043–1056
https://doi.org/10.1007/s10126-023-10258-9

RESEARCH

# Morphology, Histology, and Transcriptome Analysis of Gonadal Development in *Octopus minor* (Sasaki, 1920)

**Jiahua Li[1,2] · Xiaodong Zheng[1,2]**

Received: 14 August 2023 / Accepted: 9 October 2023 / Published online: 25 October 2023


## Abstract

*Octopus minor* is an economically important species, but little is known about the histological pattern and regulatory mechanisms during gonadal development. In this study, we investigated the annual changes in total body weight (TW), gonad somatic index (GSI), gonadal histological features, and transcriptome of *O. minor*. The results indicated that both females and males showed a similar TW trend. The GSI peaked in June in females, while it remained constant at around 3% in males. Nine and four histological stages were observed in ovaries and testes, respectively. Our field sampling results implied that *O. minor* might have overwintering periods for both eggs and larvae. Transcriptome analysis revealed that a total of 1095 and 2468 genes were significantly expressed during ovarian and testicular development, separately. Gene Ontology (GO) and Kyoto Encyclopedia of Genes and Genomes (KEGG) enrichment analysis displayed that 126 GO terms and 5 KEGG pathways were significantly enriched in the ovarian group of advanced vitellogenic oocytes vs vitellogenic oocytes (AVO vs VO). The pathways "Ribosomal", "Cell cycle", and "Progesterone-mediated oocyte maturation" were predicted to promote yolk deposition. Additionally, the testicular comparison group of spent vs mature (Spent vs Mature) showed significant enrichment in 674 GO terms and 13 KEGG pathways, suggesting that energy metabolism and cell repair pathways may be involved in the spermatogenesis process. This work revealed the development process of the gonads and shed light on the potential regulatory pathways of *O. minor*, providing novel insights and laying a molecular basis for artificial breeding.

**Keywords** *Octopus minor* · Gonadal development · Histology · Morphology · RNA-seq

## Introduction

Understanding the regulatory mechanism of gonadal development is the basis for achieving large-scale aquaculture production. Catches of cephalopods have remained at a high level over the past 20 years, reaching 3.7 million tons in 2020 (FAO 2022). Many efforts have been made to artificially breed cephalopods worldwide (Bo et al. 2014; Ibarra-García et al. 2018; Jiang et al. 2020; Meza-Buendía et al. 2021; Rodríguez et al. 2006). However, current catches and production still do not meet the demand, so there is an urgent need to develop cephalopod cultivation.

The long-armed octopus, *Octopus minor* (Sasaki, 1920), is widely distributed in the coastal waters of China, Korea, and Japan (Norman et al. 2014). As an important and promising marine mollusk in China, *O. minor* is tasty and rich in protein and multiple unsaturated fatty acids (Qian et al. 2010; Zheng et al. 2014). To date, there have been several reports on the artificial culture of *O. minor* (Bo et al. 2014, 2016; Liu 2013; Nan 2020; Qian et al. 2013, 2016; Song et al. 2018; Wu and Lv 1996; Zheng et al. 2009). Unlike many octopod species, such as *O. vulgaris* and *O. mimus*, which have a planktonic period in their life history characterized by small eggs and high fecundity (Mangold 1983; Warnke 1999), *O. minor* has relatively large eggs and low fecundity, laying 9–125 eggs per female (Qian et al. 2013). To master the reproductive strategies of cephalopods, several studies have been done on gametogenesis (de Lima et al. 2013; López-Peraza et al. 2013; Sieiro et al. 2014; Wang et al. 2015). The

✉ Xiaodong Zheng
xdzheng@ouc.edu.cn

Jiahua Li
jiahuali@stu.ouc.edu.cn

[1] Key Laboratory of Mariculture, Ministry of Education, Ocean University of China, Qingdao 266003, China

[2] Institute of Evolution and Marine Biodiversity, Ocean University of China, Qingdao 266003, China

morphology and histogenesis of gonads in *O. minor* have been reported (Li 2010; Qian et al. 2016; Xu et al. 2008), but the stage classification is still incomplete. Besides, our current understanding of the molecular reproductive profile of *O. minor* remains limited. Therefore, knowing the reproductive mechanisms is of prime importance for the artificial breeding of *O. minor*.

Omics technology has developed rapidly in recent years, offering a powerful tool for clarifying the molecular mechanisms of physiological biochemistry. Transcriptome can directly display gene expression and has been applied to study potential reproductive mechanisms of octopods in the optic lobe, white body, and gonad (Juarez et al. 2019; Lopez-Galindo et al. 2018; Ventura-Lopez et al. 2022; Wang and Ragsdale 2018). Whole genomes of nine cephalopods have been published so far (Jiang et al. 2022), providing precise molecular information. As for *O. minor*, only its whole genome study and transcriptome analysis of ammonia stress have been conducted (Kim et al. 2018; Xu and Zheng 2020), and no other omics research has been reported.

Low fecundity and long embryonic period are the two main factors that restrict *O. minor* breeding (Qian et al. 2013; Zheng et al. 2014). Figuring out the basic biology of gonads and the molecular developmental mechanisms will lay the foundation for the genetic mechanism of reproduction. Hence, this study investigated reproductive biology, containing the gonadal morphological features and histological process, and transcriptome analysis of *O. minor*, aiming to provide a molecular basis for octopus breeding.

## Material and Methods

### Sample Collection and Morphological Measuring

*O. minor* is neither an endangered nor protected species. All work followed the principles stated in the EU Directive 2010/63/EU guidelines on cephalopod use and was approved by the Institutional Animal Care and Use Committee of Ocean University of China.

From September 2020 to June 2021, a total of 210 lively and healthy *O. minor* samples were collected monthly using bottom trawl in Swan Lake (37.3°N, 122.6°E), Shandong Province, China. In addition, eleven juveniles with invisible gonads and a male juvenile weighing 27 g were collected at the same site in June 2023. For all samples with observable gonads, total body weight (TW) and gonad weight (GW) were recorded to the nearest 0.001 g. The gonad somatic index (GSI) of *O. minor* was calculated according to Wang et al. (2015): $GSI = (GW/TW) \times 100$. Mean GSI values were generated separately for males and females.

### Histological Examination and RNA Extraction

All octopuses were anesthetized in seawater-prepared 4% ethanol for 20 min based on a prior study (Butler-Struben et al. 2018). The sex of *O. minor* samples was identified by examining the right third arm, with only males having a spoon-like hectocotylus. The ovaries and testes were subsequently removed and divided into two parts. One part was fixed in Bouin's solution and preserved in 70% ethanol for histological examination, and the other part was frozen in liquid nitrogen and stored at −80 ℃ for RNA extraction.

For histological analysis, fixed gonads were dehydrated with gradient alcohol, cleared by xylene, and then embedded in paraffin. Sections of 5-μm thickness were obtained using a Leica RM 2016 rotary microtome (Shanghai, China) and then stained with hematoxylin-eosin. Finally, the prepared sections were examined and photographed with an Olympus BX 53 microscope (Olympus, Tokyo, Japan). Different cell types in ovaries and testes were identified and described based on previous research (ICES 2010; Wang et al. 2015).

After microscopic observation, it was noticed that the ovary of *O. minor* remained invisible to the naked eye, despite the oocytes having developed to the late primary oocyte (LPO) stage. Furthermore, the transition from vitellogenic oocytes (VO) to advanced vitellogenic oocytes (AVO) required about half a year. Additionally, catching female *O. minor* with fully developed eggs in the wild is quite difficult since they stay in burrows awaiting spawning. In contrast, testes have already matured when they are visible to the naked eye, so we can generally only observe the mature and spent stages. Twelve samples were chosen for RNA sequencing, comprising three replicates of the ovaries at stages of VO and AVO, and three replicates of testes at stages of mature and spent. Ovaries at VO and AVO were collected in January and April 2021, respectively, while testes at mature and spent stages were collected independently in January and May 2021. Total RNA was extracted using TRIzol reagent following the manufacturer's protocol. RNA concentration was measured by NanoDrop 2000 and RNA quality was assessed using Agilent 5400.

### cDNA Library Construction and Sequencing

Total RNA from gonads was used as input material for sample preparations. Sequencing libraries were then generated using NEBNext® UltraTM RNA Library Prep Kit for Illumina® (NEB, USA) according to the manufacturer's recommendations.

Fragmentation was carried out using divalent cations under elevated temperature in NEBNext First Strand

Synthesis Reaction Buffer (5X). For the first strand, cDNA was synthesized by random hexamer primer and M-MuLV ReverseTranscriptase (RNase H). For the second strand, cDNA synthesis was subsequently performed using DNA Polymerase I and RNase H. Remaining overhangs were converted into blunt ends by exonuclease/polymerase activities. Then 3′ ends of DNA fragments were adenylated, and NEBNext Adaptors with hairpin loop structure were ligated to prepare for hybridization. The library fragments were purified with the AMPure XP system (Beckman Coulter, Beverly, USA) for selecting cDNA fragments of preferentially 250~300 bp in length. Then USER Enzyme (NEB, USA) was used, adaptor-ligated cDNA at 37 °C for 15 min, followed by 5 min at 95 °C. PCR was then performed with Phusion High-Fidelity DNA polymerase, Universal PCR primers, and Index (X) Primer. Finally, PCR products were purified (AMPure XP system) and the quality of libraries was assessed by the Agilent Bioanalyzer 2100 system.

Index-coded samples were clustered on the cBot Cluster Generation System using TruSeq PE Cluster Kit v3-cBot-HS (Illumina) following the manufacturer's instructions. After clustering generation, the library preparations were sequenced on the Illumina Novaseq 6000 platform to generate 150-bp paired-end reads.

### Identification of Differentially Expressed Genes and Functional Enrichment Analysis

Clean data were filtered using trimmomatic (Bolger et al. 2014) to remove reads that contained adapter contamination, low-quality nucleotides, and unrecognizable nucleotides (N) from the raw data. The genome and annotation files of *O. minor* were downloaded from the GigaScience Database (http://gigadb.org/dataset/100503). HISAT2 v2.1.0 was used to build reference genome indexes (Kim et al. 2015), and then the clean data were aligned to the *O. minor* genome. FeatureCounts was applied to quantify gene expression (Liao et al. 2014). Differential expression analysis was performed by DESeq2 (Love et al. 2014). Differentially expressed genes (DEGs) were identified as those with $|\log_2(\text{FoldChange})| > 1$ and adjusted $P$-value $< 0.05$. To functionally annotate DEGs, all genes were first annotated using eggnog-mapper v2 (Cantalapiedra et al. 2021). Then the R package AnnotationForge (https://bioconductor.org/packages/AnnotationForge/) and clusterProfiler (Wu et al. 2021) were used to conduct GO and KEGG enrichment analysis.

### Validation of RNA-seq Data by qRT-PCR

Twelve differentially expressed genes related to gonadal development were validated by qRT-PCR. All primers are shown in Table S1, with *β-actin* selected as the internal control. To synthesize cDNA, the remaining RNA from 12 gonad samples after RNA-seq sequencing was used with PrimeScript RT reagent Kit (Takara, Dalian, China) according to the manufacturer's instructions. Then, qRT-PCR was performed on the LightCycler 480 real-time PCR instrument (Roche Diagnostics, Burgess Hill, UK) by Quanti-Nova SYBR Green PCR Kit (QIAGEN, Germany) in 10 µl reactions. Each reaction contained 1 µl of cDNA, 5 µl of 2 × SYBR Green PCR Master Mix, 2.6 µl of $ddH_2O$, 0.7 µl of forward primer, and 0.7 µl of reverse primer. The cycling parameters were as follows: 95 °C for 5 min, followed by 40 cycles of 95 °C for 5 s, and 60 °C for 30 s. The relative expression levels were calculated by CT methods (Schmittgen and Livak 2008).

## Results

### Annual Changes of TW and GSI

Changes in TW and GSI from September 2020 to June 2021 are shown in Fig. 1. The TW trend was consistent in both females and males and was comparable to the letter "M". There were two growing periods, one from September to December and the other from March to April (Fig. 1A). The GSI values of females showed an increasing trend, with the minimum value occurring in September and the maximum value in June of the following year. While GSI values in males fluctuated at around 3% (Fig. 1B).

The macroscopic maturity stages of females and males are presented in Fig. 1C–G. During the immature period, the female reproductive system was small and translucent with indistinct egg grains (Fig. 1C). However, in the mature stage, the female reproductive system appeared yellowish and the ovaries were significantly enlarged and fully developed. The egg grains could be observed with the naked eye, and the oviducal glands were white (Fig. 1D). Three macroscopic stages of testicular development were observed, including maturing, mature, and spent. In the maturing stage, spermatophores were presented in males (Fig. 1E). During the mature stage, two to seven spermatophores were observed (Fig. 1F). At the spent stage, the male reproductive tract was flaccid and the testes were cream yellow with 2–3 spermatophores (Fig. 1G).

### Oogenesis

According to microscopic observation, we identified 9 oocyte stages and described the characteristics as follows.

Stage 1 — Oogonia (OO): Small round cells of 11.3 to 26.9 µm diameter, with almost no cytoplasm. These cells are near the germinal cords (Fig. 2A).

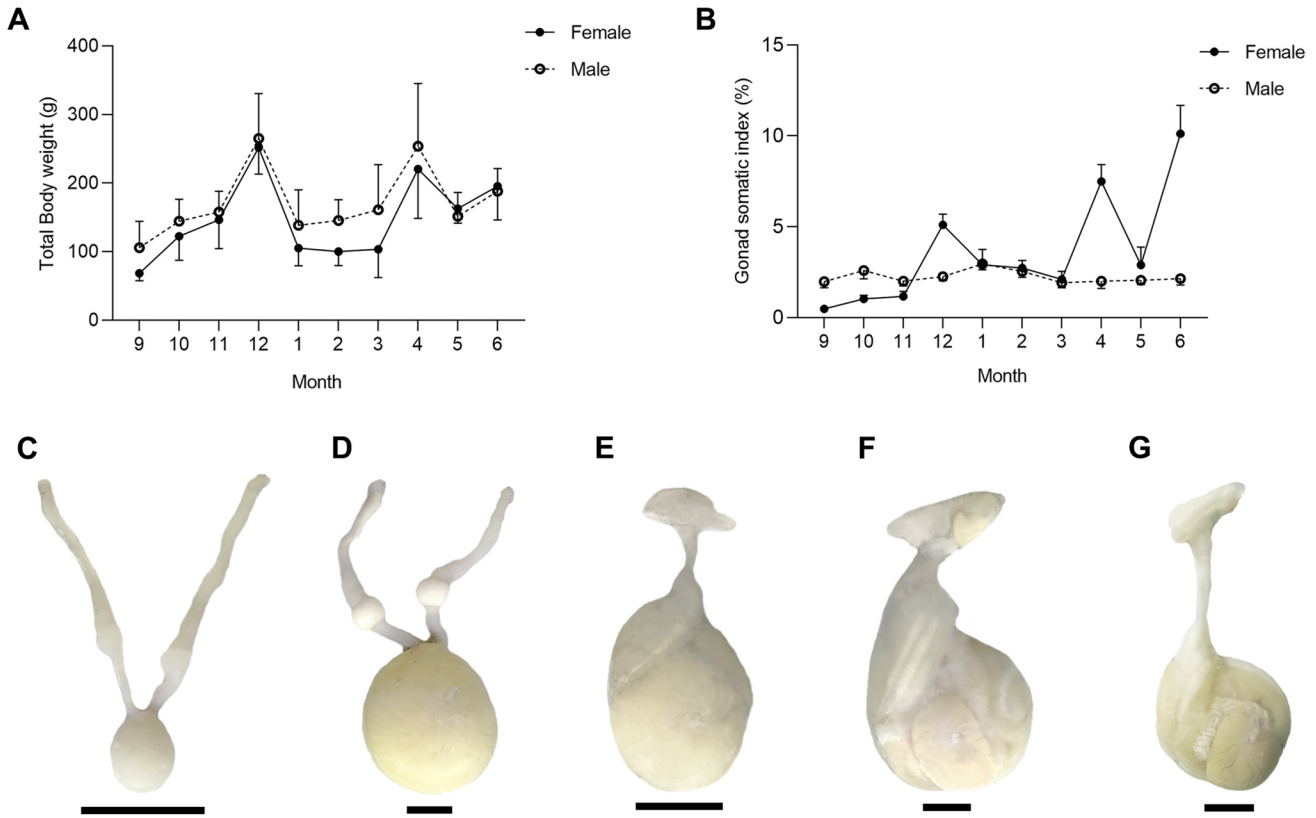


**Fig. 1** Morphological measurements and macroscopic maturity stages of *O. minor* in the male and female reproductive system. **A** Monthly change in the total body weight. **B** Monthly changes in gonad somatic index. **C** Immature ovary. **D** Mature ovary. **E** Maturing testis. **F** Mature testis. **G** Spent testis. Scale bar: **C–G** = 10 mm

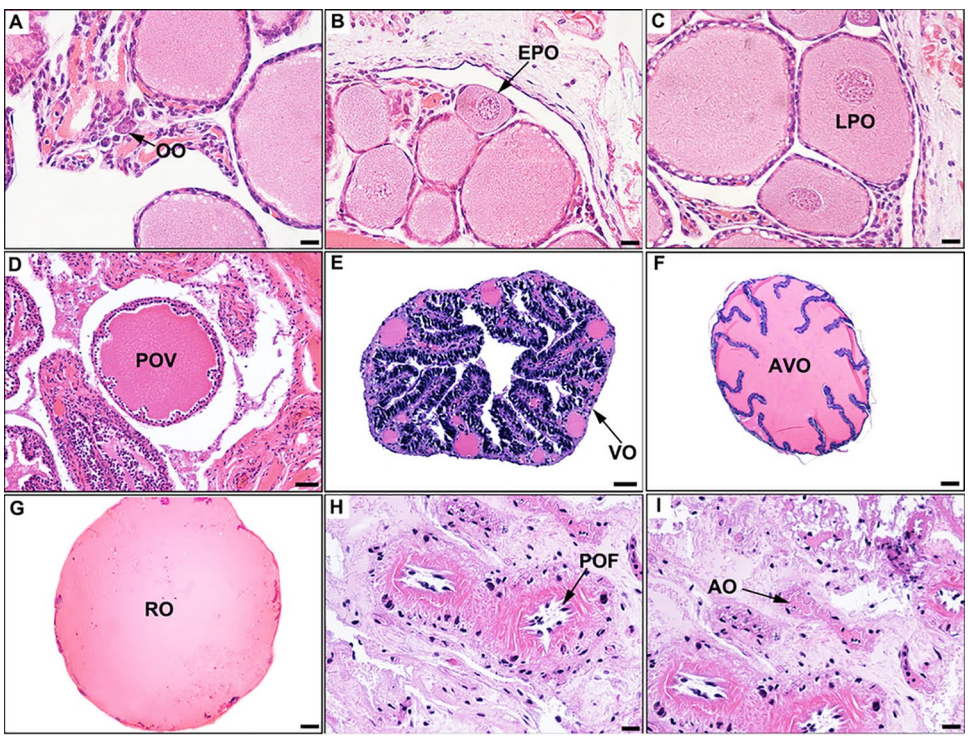


**Fig. 2** Oogenesis of ovaries in *O. minor*. **A** Oogonia (OO). **B** Early primary oocyte (EPO). **C** Late primary oocyte (LPO). **D** Previtellogenic oocyte (PVO). **E** Vitellogenic oocyte (VO). **F** Advanced vitellogenic oocyte (AVO). **G** Ripe oocyte (RO). **H** Post-ovulatory follicle (POF). **I** Atretic oocytes (AO). Scale bar: **A–C**, **H**, **I** = 20 µm; **D**, **E** = 50 µm; **F**, **G** = 200 µm

Stage 2 — Early primary oocyte (EPO): Oocytes are oval-shaped, binding to several follicles. Oocytes range from 33.8 to 74.7 μm in diameter (Fig. 2B).
Stage 3 — Late primary oocyte (LPO): Oocytes are surrounded by a layer of small follicle cells. The diameters of oocytes vary between 97.1 and 194.0 μm. The cytoplasmic portion of the cell is larger than the nucleus. Lipid inclusions can be observed in the cytoplasm (Fig. 2C).
Stage 4 — Previtellogenic oocyte (PVO): The follicle cells proliferate intensively. The follicle epithelium consists of two layers of follicular cells, with the inner layer of follicle cells forming folds and penetrating deep inside the cell. The diameter of the oocyte increases (179.6 to 394.2 μm). The nucleoli begin to degenerate, and the yolk globules are initially produced. The lipid inclusions multiply and enlarge (Fig. 2D).
Stage 5 — Vitellogenic oocyte (VO): Oocyte size increases greatly, with the diameters ranging from 235.3 to 735.2 μm. The follicular epithelium is active during vitellogenesis and chorion formation. Follicular folds migrate to the periphery of the oocyte through yolk formation (Fig. 2E).
Stage 6 — Advanced vitellogenic oocyte (AVO): Oocytes reach the maximum size (1246.1 to 3144.7 μm). The cytoplasm is filled with yolk granules and surrounded by the chorion (Fig. 2F).
Stage 7 — Ripe oocyte (RO): Oocytes are released by the preovulatory follicle. The cytoplasm contains yolk granules and the folds are completely reabsorbed, involved, and protected by the chorion. These oocytes are ready for ovulation. The oocyte diameters varied between 2187.1 and 3405.9 μm (Fig. 1G).
Stage 8 — Post-ovulatory follicle (POF): The post-ovulatory follicle is generated by the follicular epithelium after ovulation. Follicles are irregularly shaped and contain a star-shaped lumen filled with fibrous material and highly amorphous and basophilic bodies (Fig. 2H).
Stage 9 — Atretic oocyte (AO): The follicular epithelium in atretic oocytes is disorganized. The fibrillar connective tissue is replaced by collagen fibers. The chorion is disorganized and fragmented (Fig. 2I).

Four types of oocytes (OO, EPO, LPO, and RO) typically appeared in June. In September, three types of oocytes (PVO, POF, and AO) could be observed. The VO phase was the primary type of oocyte that existed from September to March of the subsequent year, while AVO mainly occurred from April to May.

## Spermatogenesis

Four microscopic stages of testicular development were observed and described below.

Stage 2a (developing): In the seminiferous tubules, spermatogonia, a large number of primary and secondary spermatocytes, and a small amount of sperm cells are observed, with the absence of spermatozoa (Fig. 3A).
Stage 2b (maturing): The seminiferous tubules are clearly defined with the presence of spermatogonia, primary and secondary spermatocytes, and spermatids. Spermatozoa are visible in all seminiferous tubules (Fig. 3B).
Stage 3a (mature): The seminiferous tubules are large and well-defined with no intercellular gap. All cell types are present, and there is an abundance of spermatozoa in the central lumen (Fig. 3C).
Stage 3b (spent): Only a limited number of primary and secondary spermatocytes, spermatids, and spermatozoa are scattered throughout the seminiferous tubules (Fig. 3D).

The developing stage of testes was observed in an octopus weighing 27 g in June, whereas the maturing stage was mainly examined in September. The mature stage was the period that lasted the longest from September to March of the following year. The spent phase primarily occurred from April to June.

## Data Quality Control and Alignment

A total of 528,428,198 raw reads were obtained from 12 gonad samples, which were divided into 4 groups: AVO, VO, Spent, and Mature. After filtering, 505,726,548 clean reads were retained. The values of Q20 (%) and Q30(%) exceeded 98.22% and 93.68% (Table S2), respectively. Clean reads were aligned to the *O. minor* genome, with overall

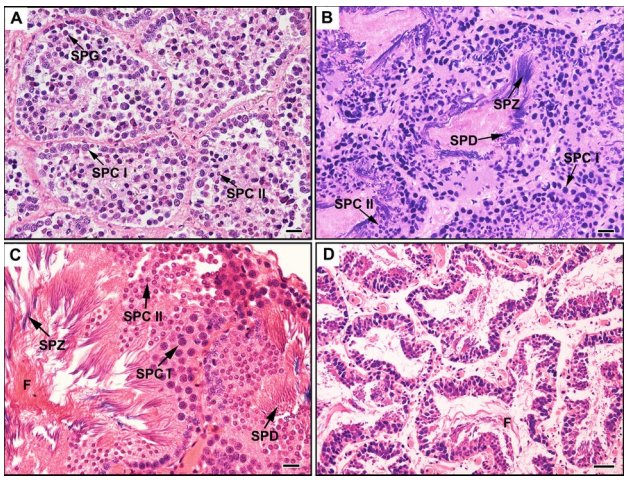


**Fig. 3** Spermatogenesis of testes in *O. minor*. **A** Developing. **B** Maturing. **C** Mature. **D** Spent. Spermatogonia (SPG), primary spermatocytes (SPC I), secondary spermatocytes (SPC II), spermatids (SPD), spermatozoa (SPZ), and flagella (F). Scale bar: **A–C** = 20 μm; **D** = 100 μm

alignment rates ranging from 76.8 to 89.9%. All raw data were submitted to the Sequence Read Archive (SRA) of the National Center for Biotechnology Information (NCBI) under the Bioproject PRJNA993392, with accession numbers SRR25224769-SRR25224780.

## Differential Expression, GO, and KEGG Enrichment Analysis

The counts obtained from FeatureCounts were utilized for differential expression analysis. In the "AVO vs VO" group, 1095 DEGs showed significantly differential expression, including 534 upregulated genes and 561 downregulated genes (Fig. 4A, B). Meanwhile, in the "Spent vs Mature" group, a total of 2468 DEGs were significantly differentially expressed, consisting of 909 upregulated genes and 1559 downregulated genes (Fig. 4A, B). Figure 4C displays the gene expression profiles of 10,175 DEGs in four groups, revealing great differences between the ovary and testis.

To explore the potential regulatory function and pathway of DEGs in gonad development, we performed the enrichment analysis. The results showed that 126 GO terms were significantly enriched in the group "AVO vs VO" (Table S3), mainly associated with biological processes such as "Cytoplasmic translation", "RNA splicing", and "G1/S transition of the mitotic cell cycle" (Fig. 5A). In the KEGG analysis, five pathways were found to be significantly enriched and downregulated, namely "Ribosome", "Cell cycle-yeast", "Cell cycle", "Progesterone-mediated oocyte maturation", and "Meiosis-yeast" (Fig. 5B, Table 1), suggesting a weakened yolk deposition activity during the further maturation of the oocytes.

The GO enrichment analysis presented that 674 GO terms of 2468 DEGs were considerably enriched in "Spent vs Mature" (Table S4). These terms primarily centered on "Meiosis", "RNA splicing", and "Regulation of cyclin-dependent protein serine/threonine kinase activity" (Fig. 6A). Thirteen KEGG pathways were significantly enriched, consisting of four upregulated DEGs pathways and nine downregulated DEGs pathways (Table 1), respectively. The pathways "Spliceosome", "mRNA surveillance pathway", "Nucleocytoplasmic transport", and "Protein processing in endoplasmic reticulum"

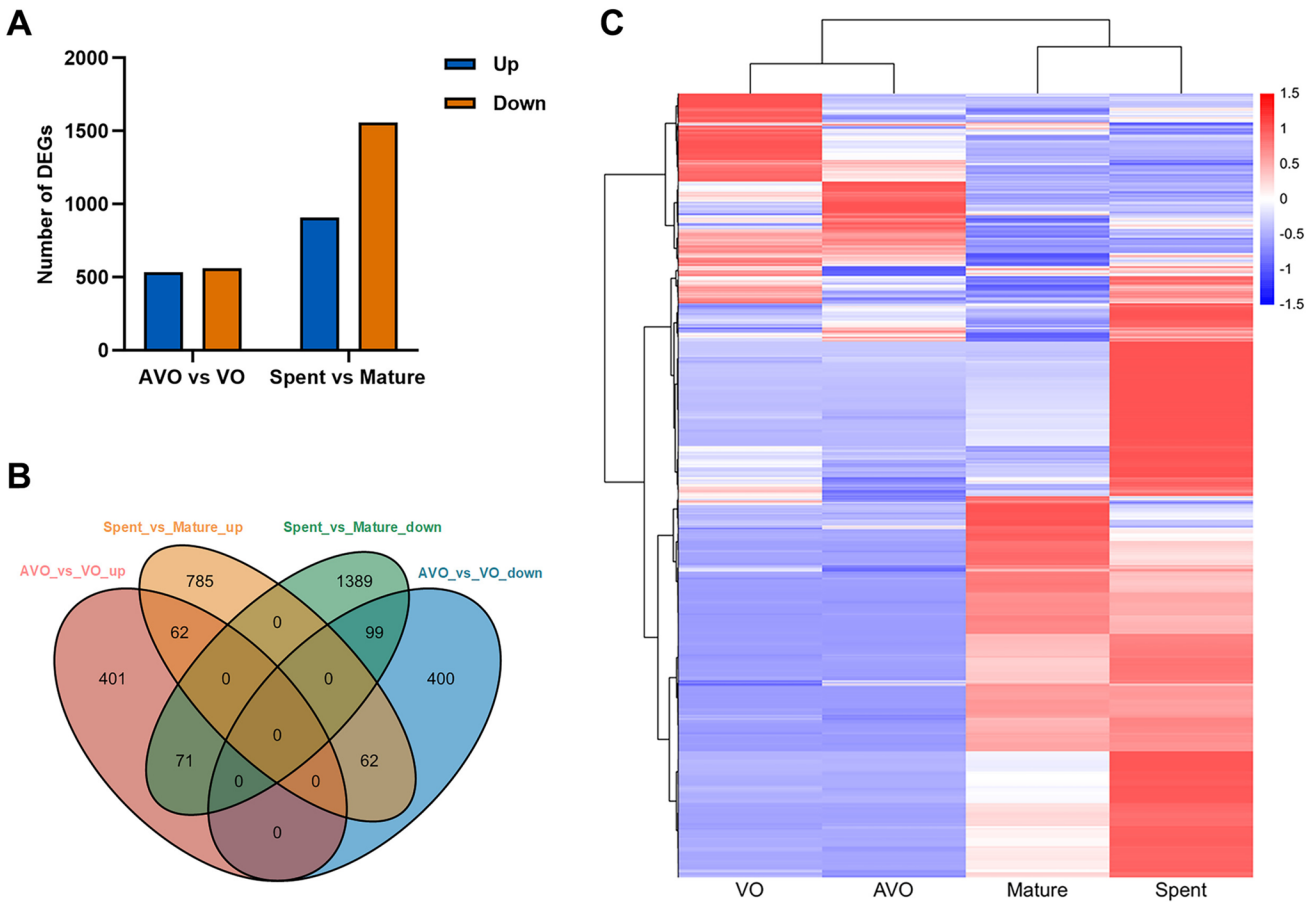


**Fig. 4** DEGs of ovaries and testis in *O. minor*. **A** Upregulated and downregulated DEGs in the ovary and testis. **B** Venn diagram of DEGs. **C** Heat map of 10,175 DEGs

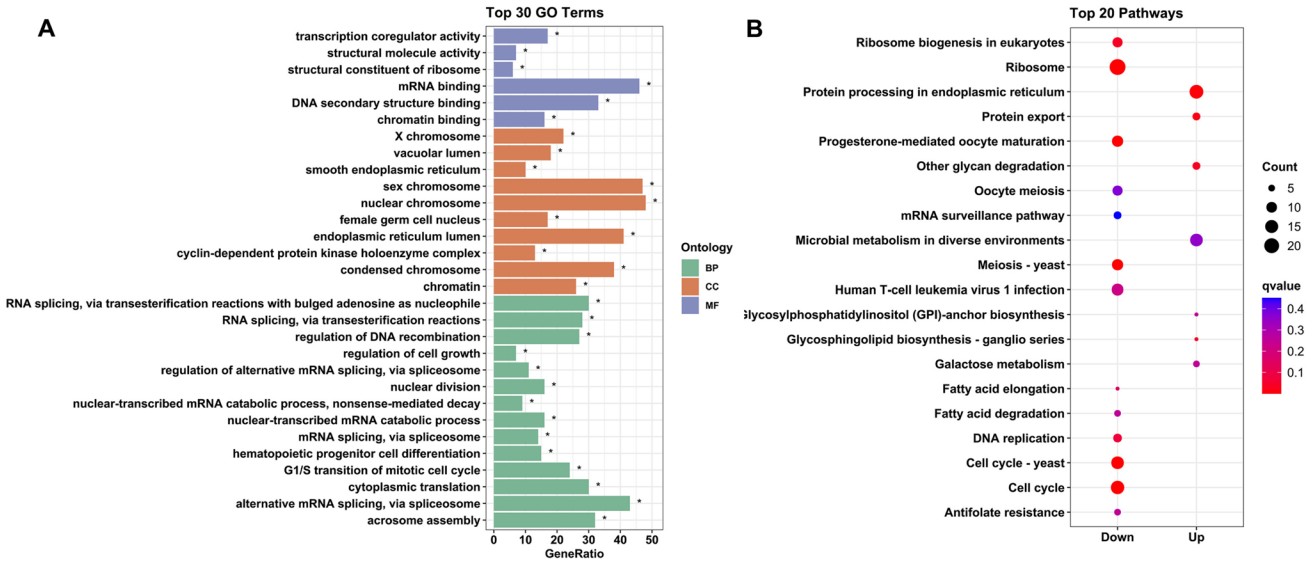


**Fig. 5** Enrichment analysis of DEGs in ovaries of *O. minor*. **A** Gene ontology (GO) annotation. **B** KEGG pathway of DEGs. Asterisks represent significantly enriched terms

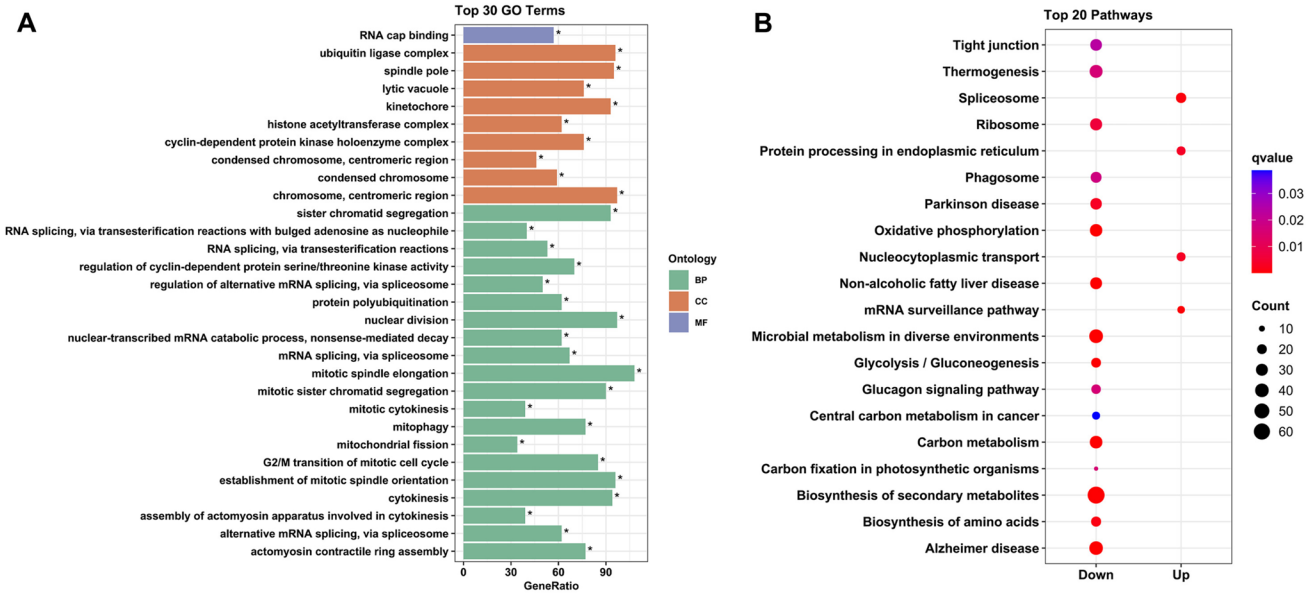


**Fig. 6** Enrichment analysis of DEGs in testes of *O. minor*. **A** Gene ontology (GO) annotation. **B** KEGG pathway. Asterisks represent significantly enriched terms

were observed to be upregulated. Meanwhile, "Oxidative phosphorylation", "Carbon metabolism", and "Glycolysis/gluconeogenesis" pathways were downregulated (Fig. 6B).

## Validation of RNA-seq Data by Quantitative Real-Time PCR

To verify the reliability of the RNA-seq data, we selected 12 genes for qRT-PCR validation, including 7 DEGs for ovaries and 5 DEGs for testes independently. Overall, the qRT-PCR results were consistent with the RNA-seq data (Fig. 7).

## Discussion

*O. minor* is an economically valuable species in northern China, but its gonadal research is currently limited. Identifying and categorizing stages of maturity is essential for artificial

**Table 1** Significantly enriched KEGG pathways in "AVO vs VO" and "Spent vs Mature"

| Group | KEGG pathway | KO number | qvalue | Input number | Regulation |
|---|---|---|---|---|---|
| AVO vs VO | Ribosome | ko03010 | 1.25E-06 | 23 | Down |
| | Cell cycle - yeast | ko04111 | 0.00016579 | 14 | Down |
| | Cell cycle | ko04110 | 0.000214682 | 16 | Down |
| | Progesterone-mediated oocyte maturation | ko04914 | 0.002116099 | 11 | Down |
| | Meiosis - yeast | ko04113 | 0.002200216 | 11 | Down |
| Spent vs Mature | Oxidative phosphorylation | ko00190 | 1.19E-06 | 33 | Down |
| | Alzheimer disease | ko05010 | 3.71E-06 | 40 | Down |
| | Carbon metabolism | ko01200 | 6.85E-06 | 34 | Down |
| | Microbial metabolism in diverse environments | ko01120 | 4.52E-05 | 41 | Down |
| | Non-alcoholic fatty liver disease | ko04932 | 8.30E-05 | 30 | Down |
| | Glycolysis/gluconeogenesis | ko00010 | 0.000110392 | 20 | Down |
| | Biosynthesis of secondary metabolites | ko01110 | 0.000110392 | 67 | Down |
| | mRNA surveillance pathway | ko03015 | 0.000416899 | 13 | Up |
| | Spliceosome | ko03040 | 0.000881029 | 22 | Up |
| | Biosynthesis of amino acids | ko01230 | 0.001274357 | 21 | Down |
| | Parkinson disease | ko05012 | 0.003201312 | 28 | Down |
| | Nucleocytoplasmic transport | ko03013 | 0.003532193 | 17 | Up |
| | Protein processing in endoplasmic reticulum | ko04141 | 0.00383301 | 17 | Up |

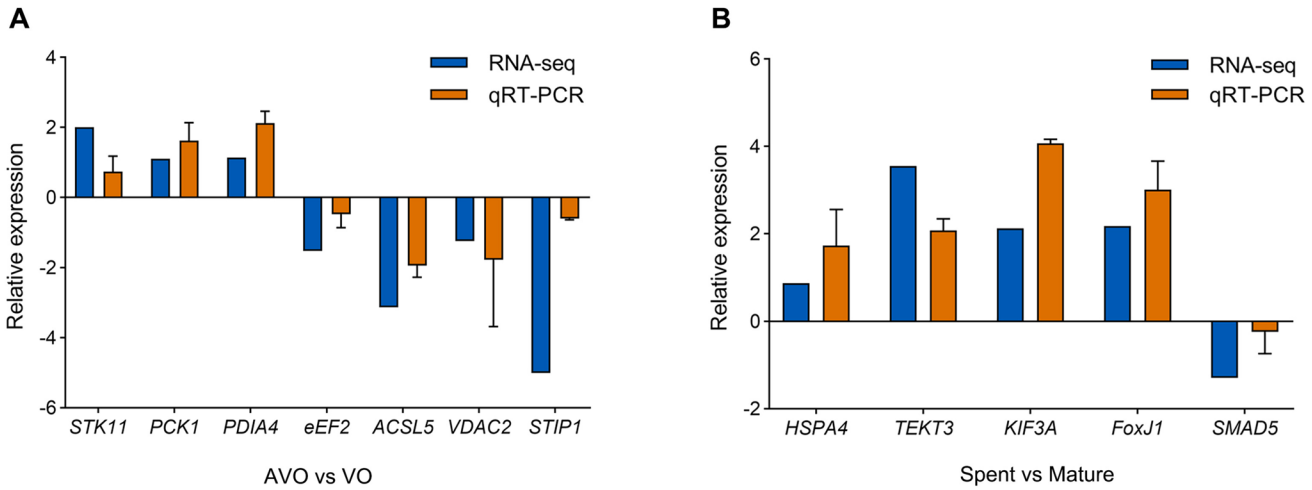


**Fig. 7** Validation of differentially expressed genes in *O. minor*. **A** Seven DEGs in group "AVO vs VO". **B** Five DGEs in "Spent vs Mature"

cultivation and fisheries. Therefore, this study investigated the histological processes of gonad development and changes in BW and GSI of both female and male *O. minor*. Additionally, we selected two key histological stages in the ovaries and testes of *O. minor* to conduct transcriptome analysis and identify potentially critical regulatory pathways and genes.

## Reproductive Strategy and Histology of Gonadal Development

Like most cephalopods, *O. minor* is a short-lived and rapidly developing species. In females, TW and GSI increased rapidly from September to December, then decreased and remained flat until March of the subsequent year. Proteins in muscle serve as the main energy reserve for cephalopods, while lipids are critical energy sources for the ovary (Rosa et al. 2004, 2005). In *O. vulgaris*, Sieiro et al. (2020) recorded a notable decline in lipids and an increase in proteins in the digestive glands of females from winter to spring, but no significant changes were observed in these two biochemical compositions in the mantle. It has been demonstrated that proteins and lipids in the mantle and digestive glands of cephalopods decrease during the period of spawning and post-spawning (Kilada and Riad 2008;

Morillo-Velarde et al. 2013). However, no relevant studies have been conducted on *O. minor*. We hypothesize that females may initially use the energy obtained from food to maintain the basic physiological metabolism, and possibly consume lipids from the digestive glands to provide energy during the overwintering period, which may explain the observed decrease and stagnation in both BW and GSI. Yolk deposition in cephalopods is a long process. Oocytes in the VO phase require around 6 months to progress to the AVO stage due to the insufficient lipid supply during the overwintering period. When temperatures rise in March, abundant food will lead to weight gain and make the ovary fuller until ovulation. In some cephalopods, females would limit the growth of somatic cells to meet reproductive development, while males may experience concurrent somatic growth with reproductive cell development (Jackson et al. 2004; Lin et al. 2015). Therefore, we speculate that this reproductive strategy also applies to *O. minor*, which may account for the higher mean BW of the males compared to the females collected simultaneously in this study.

Changes in the female reproductive system during maturation were evident. Figure 2C, D show that ovaries are much fuller and light-yellowish, and the oviducal glands significantly enlarged with the color changed from translucent to creamy white. However, this color transition of oviducal glands is different from the brown or amber color found in many other mature octopod species (de Lima et al. 2013; Olivares et al. 2017). The peripheral gland of the female reproductive system was reported to produce mucins as the ovary matures, which in turn enlarges the oviducal gland (Froesch and Marthy 1975). Additionally, we also noticed that females were generally smaller than males, probably because they allocated more energy to reproduction.

In cephalopods, it is very common that males undergo a very short sub-mature period and mature much earlier than females, with spermatophores present for most time of the year (Avila-Poveda et al. 2009; López-Peraza et al. 2013; Otero et al. 2007). Females can store sperm in oviducal glands for months (Mangold 1987), enabling males to mate with females almost all year round. In this study, we observed that the number of spermatophores ranged from 2 to 9 in male *O. minor*, which was much fewer than that of octopod species with a benthic stage like *O. vulgaris*. Besides, we found that the male *O. minor* with spermatophores weighed 32 g, indicating that juveniles are capable of mating.

The histological process of gonad development in *O. minor* is similar to other cephalopods. According to the histological classification of *O. vulgaris* (ICES 2010), nine and four stages were observed in females and males, respectively. Oocyte development in *O. minor* is asynchronous, as oocytes closer to the germinal cord mature more slowly. The appearance of the previtellogenic oocyte signifies the beginning of maturation and yolk deposition, which lasts for at least 6 months in *O. minor*. In April, spermatozoa were found in the oviducal gland of *O. minor*, whereas no spermatozoa were observed before this time, suggesting that the peak time of the mating may occur in April. The process of spermatogenesis in *O. minor* is akin to that of *O. vulgaris* and *A. fangsiao* (Cuccu et al. 2013; Wang et al. 2015). In the seminiferous tubules, the outer primary spermatocytes undergo meiosis and mitosis to produce a large number of spermatozoa in the center of the tubular lumen. As mentioned above, males matured very fast and spermatophores were observed in all 10 months of sampling from 2020 to 2021, which was in accordance with the result of other studies (Avila-Poveda et al. 2009; Cuccu et al. 2013; de Lima et al. 2013).

*O. minor* is known to spawn from July to late August (Liu 2013; Qian 2011) and incubate for 72 to 89 days under temperatures of 21 to 25 ℃ (Qian et al. 2013). Consequently, it seems reasonable to assume that *O. minor* hatchlings appear in October. However, the majority of octopuses collected in September weighed about 50 g, and the others weighed around 110 g. Previous data from artificial culture showed that *O. minor* larvae needed about 200 days to reach a weight of 50 g and 250 days to achieve 110 g under adequate food conditions (Zheng et al. 2014). However, these two results seem contradictory if the embryo development time in the wild coincides with that under artificial conditions. So, *O. minor* in Swan Lake was investigated in June 2023. As a result, eleven juveniles of 1.2 to 2.0 g were successfully captured and identified as *O. minor* by DNA barcoding. Research has indicated that an artificially hatched *O. minor* juvenile weighed 1.33 g at 75 days (Nan 2020). Therefore, it is highly likely that the juveniles in Swan Lake hatched around March. In addition to this, we also collected a larger *O. minor* weighing 27 g.

Compared to shallow waters, deep-sea water temperatures are lower. The incubation period of some deep-sea cephalopod eggs has been reported to be several years (Robison et al. 2014; Wood JB et al. 1998). Therefore, based on the current results and analysis, we hereby propose that *O. minor* has a lifespan of at least 18 months and may employ a special reproductive strategy with both egg and larval overwintering periods. In northern China, seawater temperatures gradually decrease from September and can even drop to 0 ℃ in December. The biology zero of fertilized eggs for *O. minor* was 3.79 ℃, indicating that *O. minor* could well adapt to low temperatures (Liu 2013). To make the larvae survive, *O. minor* may adopt an egg overwintering strategy; that is, fertilized eggs laid in July to August develop slowly at low temperatures and then hatch in March of the following year when the seawater temperature is suitable. After half a year, larvae would grow to 50 g by September. On the other hand, the presence of the larger juvenile suggests that *O. minor* is

likely to have a larval overwintering period as well. Briefly, fertilized eggs hatch from October to November and grow slowly at low temperatures. However, there is no observational study of *O. minor* fertilized eggs hatching in the wild, and our speculations need to be confirmed by further field research.

## Key Pathways of Ovarian Development in *O. minor*

Yolk deposition of oogenesis in cephalopod is a critical and long process that typically lasts for several months (de Lima et al. 2013; Rodríguez-Rúa et al. 2005; Wang et al. 2015). As shown in Table 1, five pathways are significantly enriched in group "AVO vs VO". A total of 75 downregulated genes were clustered in the ribosomal, cell cycle, progesterone-mediated oocyte maturation, and meiotic pathways that were highly associated with oocyte development.

Yolk in oocytes is mainly synthesized by ribosomes in follicular cells and subsequently transported to the cytoplasm of oocytes. As the oocyte matures, yolk synthesis activity gradually decreases. The KEGG result indicated that twenty-three ribosomal protein genes or rRNA molecules were enriched in the ribosomal pathway, suggesting that these *RPLs* and *RPSs* are involved in the biosynthesis of oocyte yolk, which is common in other studies (Rojo-Bartolome et al. 2016; Sun et al. 2022). The histological results showed that the follicular epithelium, composed of follicular cells, was highly active during the VO stage. As the oocytes developed into AVO, the cytoplasm was filled with yolk granules, and the ability to synthesize ribosomes was diminished.

Animals complete the first meiotic division before ovulation, in which the transition from G2 to M phase is one of the key processes in oocyte maturation. *CPEB* controls mRNA polyadenylation during oocyte maturation in the progesterone-mediated oocyte maturation pathway (Stebbins-Boaz et al. 1996), and it also increases the mitosis-promoting factor (MPF) Cdc2/cyclin B by downregulating *Myt1* (Nakajo et al. 2000). Additionally, the role of progesterone-mediated oocyte maturation in many aquatic animals is closely related to the cell cycle signaling pathway (Jia et al. 2018). In the present study, GO term cyclin-dependent protein kinase holoenzyme complex (GO: 0043073) was notably enriched, and *CDK1*, *CDC25A*, and *CCNB2* genes were upregulated in the VO stage and were co-regulated in both "Progesterone-mediated oocyte maturation" and "Cell cycle" pathways. In the "Cell cycle" pathway, *CDC25* mediates dephosphorylation to activate the CyclinB-CDK1 complex, which phosphorylates several substrates and triggers centromere segregation and chromosome condensation. Once chromosomes are condensed and aligned at the midplate, *CDK1* activity will be turned off by *WEE1*- and *PKMYT1*-mediated phosphorylation, allowing for sister chromatid separation, chromosome decondensation, reorganization of the nuclear membrane, and cytoplasmic division (Morgan 1995; Mueller et al. 1995). Our results showed that these three genes were upregulated during the VO stage, highlighting their indispensability in the yolk synthesis of *O. minor*, and suggesting that oogenesis involves a complex process of multiple factors and pathways. Also, *MCM4*, *MCM7*, *BUB1*, and *SMC1B* were upregulated in the AVO stage, indicating that they are also relevant to the cell cycle and meiosis.

## Key Pathways of Testicular Development in *O. minor*

Spermatogenesis comprises three stages, including spermatogonia mitosis, spermatocyte meiosis, and spermatocyte metamorphosis into spermatozoa. Testes classification depends on the presence and proportion of primary spermatocytes, secondary spermatocytes, spermatocytes, and spermatozoa. In the present study, the testis exhibited a more complicated developmental process, as more KEGG pathways were significantly enriched in the testes than in the ovaries.

Energy metabolism in the testis is essential for spermatozoa. In this study, we observed the significant downregulation of "Oxidative phosphorylation", "Carbon metabolism", and "Glycolysis/gluconeogenesis" pathways, which implies that the process of testis recession may be regulated by reduced energy metabolism and decreased energy supply. The "Oxidative phosphorylation" pathway is also critical for testis as it is involved in several processes, such as sperm survival, development, and motility, by functioning in the mitochondria of germ cells and supporting cells, thus affecting sperm quantity and quality (Wang et al. 2022). Like the oriental river prawn *Macrobrachium nipponense* (Jin et al. 2022), "Oxidative phosphorylation" was the most significantly enriched pathway in *O. minor* testes. ATP synthase subunits participate in the oxidative phosphorylation process of energy production in sperm mitochondria, which was found to be crucial in the formation of *Drosophila* sperm mitochondria (Sawyer et al. 2017). In this study, several ATP synthase subunit genes such as *ATP5L*, *ATP6V0C*, and *ATP5F1* were downregulated, signifying that these genes may decrease the level of energy metabolism in spermatozoa, in turn, affect sperm motility and survival. To compensate for the deficiency of oxidative phosphorylation, the glycolytic pathway can provide an adequate energy supply. Glycolysis promotes the conversion of glucose ($C_6H_{12}O_6$) to pyruvate ($CH_3COCOO^- + H^+$), releasing free energy to form the high-energy molecules ATP, and reducing nicotinamide adenine dinucleotide (Lubert 1995). Gluconeogenesis, which synthesizes glucose from non-carbohydrate precursors, is an important source when the glycolytic response is insufficient (Gerich 2010). *PGAM1* is one of the key enzymes in the glycolytic pathway and studies have suggested that it may

be related to controlling the development of spermatogenic cells (Rato et al. 2012, 2016). We also noticed other main genes of the glycolytic pathway such as *ENO2*, *GAPDH*, and *GPI* were significantly downregulated in the Spent phase, suggesting that the glycolytic pathway of these genes acts in synergy with oxidative phosphorylation to provide energy for testis development during the reproductive season.

In this study, we found that several pathways involved in cellular repair, such as "mRNA surveillance pathway", "Spliceosome", "Nucleoplasmic transport", and "Protein processing in endoplasmic reticulum", were significantly upregulated. Cell repair plays a crucial role in the restoration and protection of spermatozoa during spermatogenesis (Gunes et al. 2015). Splicing, an essential regulatory process for gene expression, involves the removal of unrelated or incorrect introns from pre-mRNA, resulting in the generation of multiple mRNA isoforms, and leading to a diverse of gene functions (Nilsen 2003; Will and Luhrmann 2011). The mRNA surveillance pathway maintains precise control over intracellular signaling and metabolism by monitoring processes such as mRNA transcription, splicing, and stability. Previous studies have demonstrated the significance of mRNA surveillance and spliceosome pathways in the maturation of spermatocytes in aquatic animals (Jin et al. 2020; Xu et al. 2015). The nucleocytoplasmic transport and protein processing in the endoplasmic reticulum signaling pathways could cooperate with various pathways, including cell cycle regulation and apoptotic response (Ferrando-May 2005; Major et al. 2011; Naidoo 2009). As an important transcription factor in the endoplasmic reticulum stress pathway, *ATF6* promotes many processes, such as endoplasmic reticulum protein folding and subsequent secretion by regulating promoter region activity and inducing cellular stress response (Wang et al. 2000). A study demonstrated that knocking out *ATF6* in mice resulted in decreased male fertility (Yu et al. 2022). Furthermore, silencing *ATF6* promotes the autophagic pathway and affects apoptosis (Liu et al. 2020). Thus, the upregulation of the *ATF6* might be associated with the reparation of declining spermatozoa and the maintenance of homeostasis. *HSP90* is a molecular chaperone that takes part in numerous cellular processes. Research has shown that knocking out the *Hsp90α* gene leads to a significant reduction in high steady-state levels of HIF-1α in the testis, preventing sperm production and causing sterility in mice (Tang et al. 2021). On the other hand, *HSP90* could also enhance glycolysis and proliferation and reduce apoptosis (Xu et al. 2017). Thus, the upregulation of *HSP90* highlighted its significant function in maintaining spermatozoa homeostasis during the spent phase of male *O. minor*. In a word, the upregulated signaling pathways collaborated to enhance cellular repair functions and maintain the homeostasis of *O. minor* testis.

## Conclusion

In this study, we provided integrated data on the morphology, histology, and transcriptome of *O. minor*. We proposed that *O. minor* had a lifespan of at least 18 months and had both eggs and larval overwintering periods. Pathways identified in two stages of ovarian development were primarily linked to the "Ribosomal", "Cell cycle", and "Progesterone-mediated oocyte maturation" pathways. Genes such as *CDK1*, *CDC25A*, and *CCNB2* were considered to play key roles in yolk deposition. Energy metabolic pathways, such as "Oxidative phosphorylation" and "Glycolysis/gluconeogenesis", may contribute to energy supply for male reproduction. Relevant genes, including those in the ATP synthase subunit family and *PGAM1*, may be involved in mediating spermatogenesis. Signaling pathways related to cell repair were important for maintaining homeostasis in the recessionary testis of *O. minor*. Our study provides the molecular basis for the artificial breeding and resource conservation of *O. minor*.

**Supplementary Information** The online version contains supplementary material available at https://doi.org/10.1007/s10126-023-10258-9.

**Acknowledgements** The authors would like to thank Mr. Li Fenghui and Mr. Cai Hui from Mashan Group Co. Ltd (Shandong Province, China) for collecting samples.

**Author Contribution** Jiahua Li: conceptualization, methodology, investigation, visualization, writing-original draft. Xiaodong Zheng: conceptualization, writing — review and editing, supervision, funding acquisition.

**Funding** This work was supported by the National Natural Science Foundation of China (No. 32170536).

**Data Availability** The datasets of this study are available from the corresponding author on reasonable request.

## Declarations

**Ethics Approval** *O. minor* is neither an endangered nor protected species. All experiments were reviewed and approved by the Institutional Animal Care and Use Committee of Ocean University of China.

**Competing Interests** The authors declare no competing interests.

## References

Avila-Poveda OH, Colin-Flores RF, Rosas C (2009) Gonad development during the early life of *Octopus maya* (Mollusca: Cephalopoda). Biol Bull 216:94–102

Bo Q, Zheng X, Gao X, Li Q (2016) Multiple paternity in the common long-armed octopus *Octopus minor* (Sasaki, 1920) (Cephalopoda: Octopoda) as revealed by microsatellite DNA analysis. Mar Ecol 37:1073–1078

Bo Q, Zheng X, Wang P, Bi K (2014) Basic growth relations in experimental rearing of newly hatchlings of *Octopus minor* (Sasaki, 1920). Oceanol Limnol Sin 45:583–588. (In Chinese)

Bolger AM, Lohse M, Usadel B (2014) Trimmomatic: a flexible trimmer for Illumina sequence data. Bioinformatics 30:2114–2120

Butler-Struben HM, Brophy SM, Johnson NA, Crook RJ (2018) In vivo recording of neural and behavioral correlates of anesthesia induction, reversal, and euthanasia in cephalopod molluscs. Front Physiol 9:109

Cantalapiedra CP, Hernandez-Plaza A, Letunic I, Bork P, Huerta-Cepas J (2021) eggNOG-mapper v2: functional annotation, orthology assignments, and domain prediction at the metagenomic scale. Mol Biol Evol 38:5825–5829

Cuccu D, Mereu M, Porcu C, Follesa MC, Cau AL, Cau A (2013) Development of sexual organs and fecundity in *Octopus vulgaris* Cuvier, 1797 from the Sardinian waters (Mediterranean Sea). Mediterr Mar Sci 14:270–277

de Lima FD, Leite TS, Haimovici M, Lins Oliveira JE (2013) Gonadal development and reproductive strategies of the tropical octopus (*Octopus insularis*) in northeast Brazil. Hydrobiologia 725:7–21

FAO (2022) The State of World Fisheries and Aquaculture 2022. Towards Blue Transformation, FAO, Rome

Ferrando-May E (2005) Nucleocytoplasmic transport in apoptosis. Cell Death Differ 12:1263–1276

Froesch D, Marthy HJ (1975) The structure and function of the oviducal gland in octopods (Cephalopoda). Proc R Soc Lond B Biol Sci 188:95–101

Gerich JE (2010) Role of the kidney in normal glucose homeostasis and in the hyperglycaemia of diabetes mellitus: therapeutic implications. Diabet Med 27:136–142

Gunes S, Al-Sadaan M, Agarwal A (2015) Spermatogenesis, DNA damage and DNA repair mechanisms in male infertility. Reprod Biomed Online 31:309–319

Ibarra-García LE, Mazón-Suástegui JM, Rosas C, Tovar-Ramírez D, Bárcenas-Pazos G, Civera-Cerecedo R, Campa-Córdova AI (2018) Morphological and physiological changes of *Octopus bimaculoides*: from embryo to juvenile. Aquaculture 497:364–372

ICES (2010) Report of the workshop on sexual maturity staging of cephalopods, 8–11 November 2010. Livorno, Italy: ICES CM 2010/ACOM:49

Jackson GD, Semmens JM, Phillips KL, Jackson CH (2004) Reproduction in the deepwater squid *Moroteuthis ingens*, what does it cost? Mar Biol 145:905–916

Jia Y, Nan P, Zhang W, Wang F, Zhang R, Liang T, Ji X, Du Q, Chang Z (2018) Transcriptome analysis of three critical periods of ovarian development in Yellow River carp (*Cyprinus carpio*). Theriogenology 105:15–26

Jiang D, Liu Q, Sun J, Liu S, Fan G, Wang L, Zhang Y, Seim I, An S, Liu X, Li Q, Zheng X (2022) The gold-ringed octopus (*Amphioctopus fangsiao*) genome and cerebral single-nucleus transcriptomes provide insights into the evolution of karyotype and neural novelties. BMC Biol 20:289

Jiang D, Zheng X, Qian Y, Zhang Q (2020) Embryonic development of *Amphioctopus fangsiao* under elevated temperatures: implications for resource management and conservation. Fish Res 225:105479

Jin S, Hu Y, Fu H, Sun S, Jiang S, Xiong Y, Qiao H, Zhang W, Gong Y, Wu Y (2020) Analysis of testis metabolome and transcriptome from the oriental river prawn (*Macrobrachium nipponense*) in response to different temperatures and illumination times. Comp Biochem Physiol D Genom Proteom 34:100662

Jin S, Zhang W, Xiong Y, Jiang S, Qiao H, Gong Y, Wu Y, Fu H (2022) Genetic regulation of male sexual development in the oriental river prawn *Macrobrachium nipponense* during reproductive vs. non-reproductive season. Aquacult Int 30:2059–2079

Juarez OE, Lopez-Galindo L, Perez-Carrasco L, Lago-Leston A, Rosas C, Di Cosmo A, Galindo-Sanchez CE (2019) *Octopus maya* white body show sex-specific transcriptomic profiles during the reproductive phase, with high differentiation in signaling pathways. PLoS ONE 14:e0216982

Kilada R, Riad R (2008) Seasonal variations in biochemical composition of *Loligo forbesi* (Cephalopoda: Loliginidae) in the Mediterranean Sea and the gulf of Suez, Egypt. J Shellfish Res 27:881–887

Kim BM, Kang S, Ahn DH, Jung SH, Rhee H, Yoo JS, Lee JE, Lee S, Han YH, Ryu KB, Cho SJ, Park H, An HS (2018) The genome of common long-arm octopus *Octopus minor*. Gigascience 7:1–7

Kim D, Langmead B, Salzberg SL (2015) HISAT: a fast spliced aligner with low memory requirements. Nat Methods 12:357–U121

Li L (2010) Studies on histology of reproductive system and cell biology on spermatogenesis and oogenesis of *Octopus variabilis*. Faculty of Life Science and Biotechnology. Ningbo University, Ningbo

Liao Y, Smyth GK, Shi W (2014) featureCounts: an efficient general purpose program for assigning sequence reads to genomic features. Bioinformatics 30:923–930

Lin D, Chen X, Chen Y, Fang Z (2015) Sex-specific reproductive investment of summer spawners of *Illex argentinus* in the southwest Atlantic. Invertebr Biol 134:203–213

Liu C (2013) Studies on culture of the life cycle of *Octopus minor* (Sasaki, 1920). Fisheries College. Qingdao: Ocean University of China.

Liu F, Chang L, Hu J (2020) Activating transcription factor 6 regulated cell growth, migration and inhibiteds cell apoptosis and autophagy via MAPK pathway in cervical cancer. J Reprod Immunol 139:103120

Lopez-Galindo L, Juarez OE, Larios-Soriano E, Del Vecchio G, Ventura-Lopez C, Lago-Leston A, Galindo-Sanchez C (2018) Transcriptomic analysis reveals insights on male infertility in *Octopus maya* under chronic thermal stress. Front Physiol 9:1920

López-Peraza DJ, Hernández-Rodríguez M, Barón-Sevilla B, Bückle-Ramirez LF (2013) Histological analysis of the reproductive system and gonad maturity of *Octopus rubescens*. Int J Morphol 31:1459–1469

Love MI, Huber W, Anders S (2014) Moderated estimation of fold change and dispersion for RNA-seq data with DESeq2. Genome Biol 15:1–21

Lubert S (1995) Glycolysis biochemistry, 4th edn. W.H. Freeman & Company, New York

Major AT, Whiley PA, Loveland KL (2011) Expression of nucleocytoplasmic transport machinery: clues to regulation of spermatogenic development. Biochim Biophys Acta 1813:1668–1688

Mangold K (1983) *Octopus vulgaris*. In: Boyle PR (ed) Cephalopod life cycles Volume I: Species accounts. Academic Press, London

Mangold K (1987) Reproduction. In: Boyle PR (ed) Cephalopod life cycles Volume II: Comparative reviews. Academic Press, London

Meza-Buendía AK, Trejo-Escamilla I, Piu M, Caamal-Monsreal C, Rodríguez-Fuentes G, Diaz F, Re D, Galindo-Sánchez CE, Rosas C (2021) Why high temperatures limit reproduction in cephalopods? The case of *Octopus maya*. Aquacult Res 52:5111–5123

Morgan D (1995) Principles of CDK regulation. Nature 374:131–134

Morillo-Velarde PS, Valverde JC, Serra Llinares RM, García BG (2013) Changes in lipid composition of different tissues of common octopus (*Octopus vulgaris*) during short-term starvation. Aquacult Res 44:1177–1189

Mueller PR, Coleman TR, Kumagai A, Dunphy WG (1995) Myt1: a membrane-associated inhibitory kinase that phosphorylates Cdc2 on both threonine-14 and tyrosine-15. 270:86–90

Naidoo N (2009) ER and aging-protein folding and the ER stress response. Ageing Res Rev 8:150–159

Nakajo N, Yoshitome S, Iwashita J, Iida M, Uto K, Ueno S, Sagata N (2000) Absence of Wee1 ensures the meiotic cell cycle in *Xenopus* oocytes. Genes Dev 14:328–338

Nan Z (2020) Studies on genetic diversity located in the Bohai and Yellow Seas and artificial reproductive technique of *Octopus minor*. Fisheries college. Ocean University of China, Qingdao

Nilsen TW (2003) The spliceosome: the most complex macromolecular machine in the cell? BioEssays 25:1147–1149

Norman MD, Finn JK, Hochberg FG (2014) Family Octopodidae. In: Jereb P, Roper CFE, Norman MD, Finn JK (eds) Cephalopods of the world: an annotated and illustrated catalogue of cephalopod species known to date Volume 3 Octopods and vampire squids FAO Species Catalogue for Fishery Purposes. FAO, Rome

Olivares A, Avila-Poveda OH, Leyton V, Zuñiga O, Rosas C, Northland-Leppe I (2017) Oviducal glands throughout the gonad development stages: a case study of *Octopus mimus* (Cephalopoda). Molluscan Res 37:229–241

Otero J, González ÁF, Sieiro MP, Guerra Á (2007) Reproductive cycle and energy allocation of *Octopus vulgaris* in Galician waters, NE Atlantic. Fish Res 85:122–129

Qian Y (2011) Studies on ecological habit and artificial reproductive technique of *Octopus minor*. Fisheries College. Ocean University of China, Qingdao

Qian Y, Zheng X, Liu C, Wang P, Li Q (2013) Studies on the reproductive habit and embryonic development of *Octopus minor* under the artificial conditions. Oceanol Limnol Sin 44:583–588. (In Chinese)

Qian Y, Zheng X, Wang P, Li Q (2010) Analysis and evaluation of nutritive composition of *Octopus minor* in Lake Swan. Mar Sci 34:14–18. (In Chinese)

Qian Y, Zheng X, Wang W, Yang J, Li Q (2016) Ultrastructure of spermatozoa and spermatogenesis in *Octopus minor* (Sasaki, 1920) (Cephalopoda: Octopoda). J Nat Hist 50:2037–2047

Rato L, Alves MG, Socorro S, Duarte AI, Cavaco JE, Oliveira PF (2012) Metabolic regulation is important for spermatogenesis. Nat Rev Urol 9:330–338

Rato L, Meneses MJ, Silva BM, Sousa M, Alves MG, Oliveira PF (2016) New insights on hormones and factors that modulate Sertoli cell metabolism. Histol Histopathol 31:499–513

Robison B, Seibel B, Drazen J (2014) Deep-sea octopus (*Graneledone boreopacifica*) conducts the longest-known egg-brooding period of any animal. PLoS ONE 9:e103437

Rodríguez C, Carrasco JF, Arronte JC, Rodríguez M (2006) Common octopus *Octopus vulgaris* (Cuvier, 1797) juvenile ongrowing in floating cages. Aquaculture 254:293–300

Rodríguez-Rúa A, Pozuelo I, Prado MA, Gómez MJ, Bruzón MA (2005) The gametogenic cycle of *Octopus vulgaris* (Mollusca: Cephalopoda) as observed on the Atlantic coast of Andalusia (south of Spain). Mar Biol 147:927–933

Rojo-Bartolome I, Diaz De Cerio O, Diez G, Cancio I (2016) Identification of sex and female's reproductive stage in commercial fish species through the quantification of ribosomal transcripts in gonads. PLoS ONE 11:e0149711

Rosa R, Costa PR, Pereira J, Nunes ML (2004) Biochemical dynamics of spermatogenesis and oogenesis in *Eledone cirrhosa* and *Eledone moschata* (Cephalopoda: Octopoda). Comp Biochem Physiol B Biochem Mol Biol 139:299–310

Rosa R, Pereira J, Nunes ML (2005) Biochemical composition of cephalopods with different life strategies, with special reference to a giant squid, *Architeuthis* sp. Mar Biol 146:739–751

Sawyer EM, Brunner EC, Hwang Y, Ivey LE, Brown O, Bannon M, Akrobetu D, Sheaffer KE, Morgan O, Field CO, Suresh N, Gordon MG, Gunnell ET, Regruto LA, Wood CG, Fuller MT, Hales KG (2017) Testis-specific ATP synthase peripheral stalk subunits required for tissue-specific mitochondrial morphogenesis in Drosophila. BMC Cell Biol 18:16

Schmittgen TD, Livak KJ (2008) Analyzing real-time PCR data by the comparative C(T) method. Nat Protoc 3:1101–1108

Sieiro P, Otero J, Aubourg SP (2020) Biochemical composition and energy strategy along the reproductive cycle of female *Octopus vulgaris* in Galician waters (NW Spain). Front Physiol 11:760

Sieiro P, Otero J, Guerra Á (2014) Contrasting macroscopic maturity staging with histological characteristics of the gonads in female *Octopus vulgaris*. Hydrobiologia 730:113–125

Song M, Wang J, Zheng X (2018) Prey preference of the common long-armed octopus *Octopus minor* (Cephalopoda: Octopodidae) on three different species of bivalves. J Oceanol Limnol 37:1595–1603

Stebbins-Boaz B, Hake LE, Richter JD (1996) CPEB controls the cytoplasmic polyadenylation of cyclin, Cdk2 and c-mos mRNAs and is necessary for oocyte maturation in *Xenopus*. EMBO J 15:2582–2592

Sun R, Liu J, Xu Y, Jiang L, Li Y, Zhong G, Yi X (2022) Genome-wide identification and stage-specific expression profile analysis reveal the function of ribosomal proteins for oogenesis of *Spodoptera litura*. Front Physiol 13:943205

Tang X, Chang C, Hao M, Chen M, Woodley DT, Schönthal AH, Li W (2021) Heat shock protein-90alpha (Hsp90α) stabilizes hypoxia-inducible factor-1α (HIF-1α) in support of spermatogenesis and tumorigenesis. Cancer Gene Ther 28:1058–1070

Ventura-Lopez C, Lopez-Galindo L, Rosas C, Sanchez-Castrejon E, Galindo-Torres P, Pascual C, Rodriguez-Fuentes G, Juarez OE, Galindo-Sanchez CE (2022) Sex-specific role of the optic gland in *Octopus maya*: A transcriptomic analysis. Gen Comp Endocrinol 320:114000

Wang W, Dong G, Yang J, Zheng X, Wei X, Sun G (2015) The development process and seasonal changes of the gonad in *Octopus ocellatus* Gray off the coast of Qingdao, Northeast China. Fish Sci 81:309–319

Wang X, Yin L, Wen Y, Yuan S (2022) Mitochondrial regulation during male germ cell development. Cell Mol Life Sci 79:91

Wang Y, Shen J, Arenzana N, Tirasophon W, Kaufman RJ, Prywes R (2000) Activation of ATF6 and an ATF6 DNA binding site by the endoplasmic reticulum stress response. J Biol Chem 275:27013–27020

Wang ZY, Ragsdale CW (2018) Multiple optic gland signaling pathways implicated in octopus maternal behaviors and death. J Exp Biol 221:jeb185751

Warnke K (1999) Observations on the embryonic development of *Octopus mimus* (Mollusca: Cephalopoda) from Northern Chile. Veliger 42:211–217

Will CL, Luhrmann R (2011) Spliceosome structure and function. Cold Spring Harb Perspect Biol 3:a003707

Wood JB, Kenchington E, Rk OD (1998) Reproduction and embryonic development time of *Bathypolypus arcticus*, a deep-sea octopod. Malacologia 39:11–19

Wu C, Lv Y (1996) Behavioral habits and tolerance to water quality changes of temporary rearing *Octopus minor*. Fujian Fish 25–29. (In Chinese)

Wu T, Hu E, Xu S, Chen M, Guo P, Dai Z, Feng T, Zhou L, Tang W, Zhan L, Fu X, Liu S, Bo X, Yu G (2021) clusterProfiler 4.0: a universal enrichment tool for interpreting omics data. Innovation 2:100141

Xu K, Wen M, Duan W, Ren L, Hu F, Xiao J, Wang J, Tao M, Zhang C, Wang J, Zhou Y, Zhang Y, Liu Y, Liu S (2015) Comparative analysis of testis transcriptomes from triploid and fertile diploid cyprinid fish. Biol Reprod 92:95

Xu Q, Tu J, Dou C, Zhang J, Yang L, Liu X, Lei K, Liu Z, Wang Y, Li L, Bao H, Wang J, Tu K (2017) HSP90 promotes cell glycolysis, proliferation and inhibits apoptosis by regulating PKM2 abundance via Thr-328 phosphorylation in hepatocellular carcinoma. Mol Cancer 16:1–16

Xu R, Zheng X (2020) Hemocytes transcriptomes reveal metabolism changes and detoxification mechanisms in response to ammonia stress in *Octopus minor*. Ecotoxicology 29:1441–1452

Xu X, Yan B, Zheng J, Wang G, Cheng K (2008) Morphology and histology of the reproductive system in *Octopus variabilis*. Chin J Zool 43:77–84. (In Chinese)

Yu R, Chen X, Zhu X, He B, Lu C, Liu Y, Xu X, Wu X (2022) ATF6 deficiency damages the development of spermatogenesis in male *Atf6* knockout mice. Andrologia 54:e14350

Zheng W, Yan B, Li S (2009) Artificial seedling of octopus *Octopus variabilis*. Fish Sci 28:176–178. (In Chinese)

Zheng X, Qian Y, Liu C (2014) *Octopus minor*. In: Iglesias J, Fuentes L, Villanueva R (eds) Cephalopod culture. Springer, New York